CP violation in the interference between $\rho(770)^0$ and S-wave in $B^\pm \to \pi^+\pi^-\pi^\pm$ decays and its implication for CP asymmetry in $B^\pm \to \rho^0\pi^\pm$

Hai-Yang Cheng

Institute of Physics, Academia Sinica, Taipei, Taiwan 115, Republic of China

The decay amplitude analyses of $B^\pm \to \pi^+\pi^-\pi^\pm$ decays in the Dalitz plot performed by LHCb indicate that CP asymmetry for the dominant quasi-two-body decay $B^\pm \to \rho(770)^0\pi^\pm$ was found to be consistent with zero in all three approaches for the S-wave component and that CP-violation effects related to the interference between the $\rho(770)^0$ resonance and the S-wave were clearly observed. We show that the nearly vanishing CP violation in $B^\pm \to \rho^0\pi^\pm$ is understandable within the framework of QCD factorization. There are two $1/m_b$ power corrections, one from penguin annihilation and the other from hard spectator interactions. They contribute destructively to $\mathcal{A}_{CP}(B^\pm \to \rho^0\pi^\pm)$ to render it compatible with zero, in contrast to the sizable negative CP asymmetry predicted in most of the existing models. We next show that the measured interference pattern between the ρ and S-wave contributions in the low $m_{\pi^+\pi^-}$ region separated by the sign of value of $\cos\theta$ with θ being the angle between the two same charged pions measured in the rest frame of the ρ resonance can be explained in terms of the smallness of $\mathcal{A}_{CP}(B^+ \to \rho^0\pi^+)$ and the interference between $\rho(770)$ and $\sigma/f_0(500)$. If CP asymmetry in $B^\pm \to \rho^0\pi^\pm$ is not negligible as predicted in many existing models, the observed interference pattern will be destroyed. We conclude that the experimental observation of the interference pattern between P- and S-waves in the low-$m_{\pi^+\pi^-}$ region between 0.5 and 1.0 GeV is consistent with a nearly vanishing CP violation in $B^\pm \to \rho^0\pi^\pm$.

I. INTRODUCTION

Recently, the full amplitude analysis of $B^\pm \to \pi^+\pi^-\pi^\pm$ in the Dalitz plot has been performed by LHCb [1,2]. In this analysis, the S-wave component of $B^\pm \to \pi^+\pi^-\pi^\pm$ was studied using three different approaches: the isobar model, the K-matrix model, and a quasi-model-independent binned approach. In the isobar model, the S-wave amplitude was presented by LHCb as a coherent sum of the σ [or $f_0(500)$] meson contribution and a $\pi\pi \leftrightarrow K\bar{K}$ rescattering amplitude in the mass range $1.0 < m_{\pi^+\pi^-} < 1.5$ GeV. The fit fraction of the S-wave is about 25% and predominated by the σ resonance.

In the low invariant-mass $m(\pi^+\pi^-)_{\text{low}}$ region, CP asymmetries were clearly seen in $B^\pm \to \pi^+\pi^-\pi^\pm$ decays in the following places: (i) a significant CP violation of 15% in $B^\pm \to \sigma\pi^\pm$ implied in the isobar model, (ii) a large CP asymmetry of order 45% in the rescattering amplitude,

(iii) a CP violation of 40% in the mode with the tensor resonance $f_2(1270)$, and (iv) large CP-violating effects related to the interference between the P- and S-wave contributions with the significance exceeding 25σ in all the S-wave models. More precisely, the interference between S- and P-waves is clearly visible in Fig. 1, where the data are separated by the sign of the value of $\cos\theta_{\text{hel}}$ with θ_{hel} being the helicity angle, evaluated in the $\pi^+\pi^-$ rest frame, between the pion with opposite charge to the B and the third pion from the B decay (see Fig. 2).[1] In contrast, CP asymmetry for the dominant quasi-two-body decay mode $B^\pm \to \rho(770)^0\pi^\pm$ was found by LHCb to be compatible with zero in all three S-wave approaches.

We notice two salient features in Fig. 1: (i) CP violation in the $\rho(770)$ region is proportional to $(m_{\text{low}}^2 - m_\rho^2)\cos\theta_{\text{hel}}$ as the sign of CP asymmetry is flipped below and above the $\rho(770)$ peak and from negative $\cos\theta_{\text{hel}}$ to positive $\cos\theta_{\text{hel}}$. Hence, CP asymmetry in this region arises from the interference between the $\rho(770)$ and S-wave contributions because the angular distribution of $\rho \to \pi^+\pi^-$ is proportional to $\cos\theta_{\text{hel}}$, while it is a constant for $S \to \pi^+\pi^-$.

---

[1]The same effect also can be seen in Fig. 3 of Ref. [1], where CP asymmetries are plotted as a function of $\cos\theta_{\text{hel}}$ in regions below and above the $\rho(770)$ resonance pole.
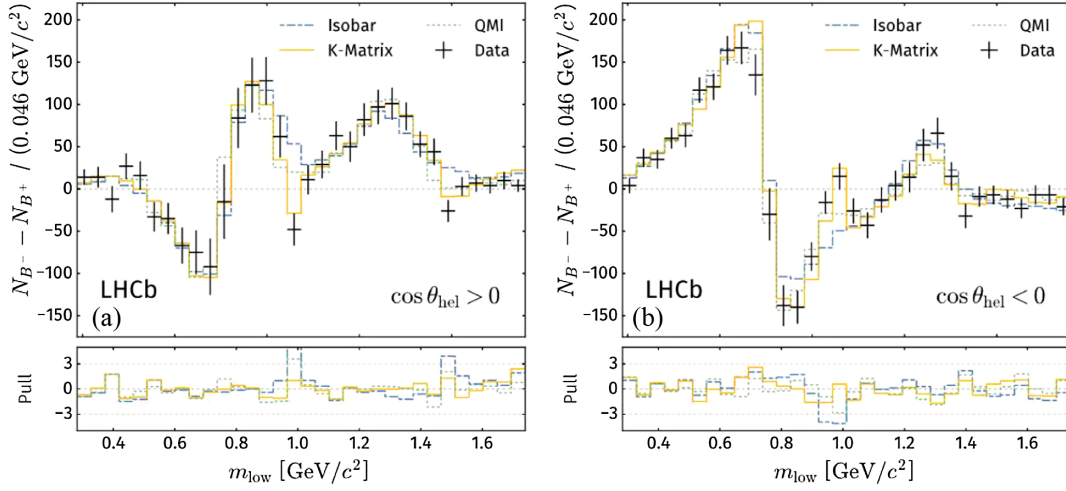
FIG. 1. The difference of N_{B^-} and N_{B^+}, the number of B^- and B^+ events, respectively, for $B^\pm \to \pi^+\pi^-\pi^\pm$ measured in the low-$m_{\pi^+\pi^-}$ region for (a) $\cos\theta_{\rm hel} > 0$ and (b) $\cos\theta_{\rm hel} < 0$ with the helicity angle $\theta_{\rm hel}$ being defined in Fig. 2. This plot is taken from Ref. [2].
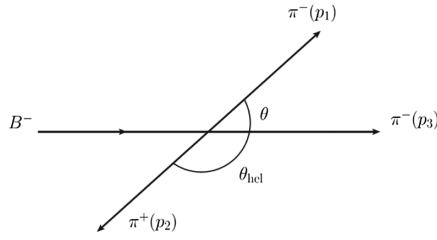

FIG. 2. The angle θ between the momenta of the two π^- pions measured in the rest frame of the dipion system in the decay $B^- \to \pi^-(p_1)\pi^+(p_2)\pi^-(p_3)$. It is related to the helicity angle $\theta_{\rm hel}$ defined by the LHCb through the relation $\theta + \theta_{\rm hel} = \pi$.

The change of asymmetry below and above the $\rho(770)$ peak implies a strong phase arising from the ρ line shape. (ii) The height of the peak and the depth of the valley near the ρ mass region are similar though the former is slightly larger than the latter.

To describe the observed interference pattern, we consider the interference between $\rho(770)$ and $\sigma(500)$ as the S-wave is predominated by the σ resonance in the isobar model. Writing

$$A_\pm \equiv A_\pm^\rho + A_\pm^\sigma = c_\pm^\rho F_\rho^{\rm BW} \cos\theta + c_\pm^\sigma F_\sigma^{\rm BW} \quad (1.1)$$

for the B^+ and B^- decays, where $A_\pm^{\rho(\sigma)} \equiv A(\mathcal{B}^\pm \to \rho^0(\sigma)\pi^\pm \to \pi^-(p_1)\pi^+(p_2)\pi^\pm(p_3))$, $F_\rho^{\rm BW}$ and $F_\sigma^{\rm BW}$ are the Breit-Wigner propagators of the $\rho(770)$ and σ, respectively, for example,

$$F_\rho^{\rm BW}(s_{12}) = \frac{1}{s_{12} - m_\rho^2 + im_\rho\Gamma_\rho}. \quad (1.2)$$

We use the Breit-Wigner line shape for the purpose of illustration. In realistic calculations given in Sec. IV below, we shall utilize the Gounaris-Sakurai model to describe the line shape of the $\rho(770)$ meson and the pole model for the σ resonance. In Eq. (1.1), we have followed Ref. [3] to define the quantity θ being the angle between the two same charged pions measured in the rest frame of the dipion system (i.e., the resonance). This angle is related to the helicity angle $\theta_{\rm hel}$ defined by LHCb [2] through the relation $\theta_{\rm hel} + \theta = \pi$ (see Fig. 2). Hence, $\cos\theta_{\rm hel} = -\cos\theta$.

It follows that CP asymmetry has the expression,

$$
\begin{aligned}
\mathcal{A}_{CP} &\propto |A_-|^2 - |A_+|^2 \\
&= (|c_-^\rho|^2 - |c_+^\rho|^2)|F_\rho^{\rm BW}(s_{12})|^2 \cos\theta^2 + (|c_-^\sigma|^2 - |c_+^\sigma|^2)|F_\sigma^{\rm BW}(s_{12})|^2 \\
&\quad + 2|F_\rho^{\rm BW}(s_{12})|^2|F_\sigma^{\rm BW}(s_{12})|^2 \cos\theta\{{\rm Re}(c_-^{*\rho}c_-^\sigma - c_+^\rho c_+^{*\sigma})[(s_{12} - m_\rho^2)(s_{12} - m_\sigma^2) \\
&\quad + (m_\rho\Gamma_\rho)(m_\sigma\Gamma_\sigma)] + {\rm Im}(c_-^{*\rho}c_-^\sigma + c_+^\rho c_+^{*\sigma})[m_\rho\Gamma_\rho(s_{12} - m_\sigma^2) - m_\sigma\Gamma_\sigma(s_{12} - m_\rho^2)]\}. \quad (1.3)
\end{aligned}
$$

The terms $(s - m_{\rho(\sigma)}^2)$ and $m_{\rho(\sigma)}\Gamma_{\rho(\sigma)}$ arise from the real and imaginary parts, respectively, of the Breit-Wigner propagator $F_{\rho(\sigma)}^{\rm BW}(s)$. The observed interference pattern shown in Fig. 1 in the ρ mass region indicates that it is mainly governed by the $(s_{12} - m_\rho^2)\cos\theta$ term. This requires that CP violation induced by the ρ meson is negligible; that is $|c_-^\rho|^2 \approx |c_+^\rho|^2$, and that the pattern is not significantly affected by the CP asymmetry induced by σ in the region

of interest. A nearly vanishing *CP* violation originating from ρ is consistent with the fact that the *CP*-violating effect cancels when integrating over the angle. In other words, the observed interference pattern between ρ and *S*-wave is consistent with the smallness of *CP* violation in $B^{\pm} \to \rho^0 \pi^{\pm}$.

It is a long-standing puzzle in regard to the *CP* asymmetry in $B^{\pm} \to \rho^0 \pi^{\pm}$. The existing theoretical predictions based on QCD factorization (QCDF) [4,5], perturbative QCD (pQCD) [6,7], soft-collinear effective theory (SCET) [8], topological diagram approach (TDA) [9,10] all lead to a negative *CP* asymmetry for $B^{\pm} \to \rho^0 \pi^{\pm}$ except the pQCD calculation in [7], ranging from -7% to -45% [see Eq. (2.3) below].

The purpose of this work is twofold. First, we would like to point out that the nearly vanishing *CP* violation in $B^{\pm} \to \rho^0 \pi^{\pm}$ is understandable in the framework of QCDF. Second, we will present a study of *CP* asymmetries in the low-$m_{\pi\pi}$ region between 0.5 and 1.0 GeV and show that the interference pattern depicted in Fig. 1 can be explained provided that *CP* violation in $B^{\pm} \to \rho^0 \pi^{\pm}$ is negligible.

This paper is organized as follows. In Sec. II, we study *CP* violation in $B^{\pm} \to \rho^0 \pi^{\pm}$ decays in the framework of

QCDF. We then proceed to the $B^{\pm} \to \sigma \pi^{\pm}$ decays in Sec. III. In Sec. IV, we consider the three-body decays $B^{\pm} \to \pi^- \pi^+ \pi^{\pm}$ mediated by the $\rho(770)$ and $\sigma(500)$ resonances and study their interference. We summarize our results in Sec. V.

II. $B^{\pm} \to \rho^0 \pi^{\pm}$ DECAYS

CP asymmetry in the quasi-two-body decay $B^{\pm} \to \rho^0 \pi^{\pm}$ was found by LHCb to be consistent with zero in all three *S*-wave approaches [1,2]. In the isobar model,

$$\mathcal{A}_{CP}(B^+ \to \rho^0 \pi^+) = (0.7 \pm 1.1 \pm 0.6 \pm 1.5)\%, \text{ LHCb 2020.}$$
(2.1)

Recently, this asymmetry was measured by LHCb based on a method that does not require full amplitude analysis [11]. The result is

$$\mathcal{A}_{CP}(B^+ \to \rho^0 \pi^+) = (-0.4 \pm 1.7)\%, \text{ LHCb 2022.} \quad (2.2)$$

Predictions of *CP* violation (in %) in various approaches are summarized as follows:

$$\mathcal{A}_{CP}(B^+ \to \rho^0 \pi^+) = \begin{cases} \text{QCDF:} & -9.8^{+3.4+11.4}_{-2.6-10.2} \, [4], & -6.7^{+0.2+3.2}_{-0.2-3.7} \, [5] \\ \text{pQCD:} & -27.5^{+2.5}_{-3.3} \pm 1.7 \, [6], & +14.9^{+0.4+0.5}_{-0.4-0.6} \, [7] \\ \text{SCET:} & -19.2^{+15.5+1.7}_{-13.4-1.9} \, [8], & -10.8^{+13.1+0.9}_{-12.7-0.7} \, [8] \\ \text{TDA:} & -23.9 \pm 8.4 \, [9], & -45 \pm 4 \, [10] \end{cases}$$
(2.3)

Hence, except the pQCD calculation in [7] all the existing models predict a negative *CP* asymmetry ranging from -7% to -45%.

It has been claimed in [12] that in $B \to PV$ decays with $m_V < 1$ GeV, *CP* asymmetry induced from a short-distance mechanism is suppressed by the *CPT* constraint. *CPT* theorem generally implies the same lifetimes for both particle and antiparticle. When partial widths are summed over, the total width of the particle and its antiparticle should be the same. Final-state interactions are responsible

for distributing the *CP* asymmetry among the different conjugate decay channels. In the three-body *B* decays, the "$2 + 1$" approximation is usually assumed so that the resonances produced in heavy meson decays do not interact with the third particle. Within the "$2 + 1$" approximation, the observation of a large negative *CP* asymmetry of order -27% for the $B^0 \to K^*(892)^+ \pi^-$ decay with $K^*(892)^+ \to K^0 \pi^+$ [13] is compensated by a similarly large positive *CP* asymmetry in the channel $B^0 \to K^*(892)^+ \pi^-$ followed by $K^*(892)^+ \to K^+ \pi^0$; that is [14],

$$\mathcal{A}_{CP}(B^0 \to K^*(892)^+ \pi^- \to K^+ \pi^0 \pi^-) \approx -\mathcal{A}_{CP}(B^0 \to K^*(892)^+ \pi^- \to K^0 \pi^+ \pi^-) \quad (2.4)$$

This can be tested once *CP* asymmetry in $B^0 \to K^0 \pi^+ \pi^-$ is measured in the future. Likewise, $\mathcal{A}_{CP}(B^+ \to \rho^0 \pi^+ \to \pi^+ \pi^- \pi^+)$ is expected to vanish as the ρ^0 cannot decay into two neutral pions. By the same token, one will also expect a vanishing $\mathcal{A}_{CP}(B^+ \to \rho^0 K^+ \to \pi^+ \pi^- K^+)$. However, this is in contradiction to the experimental observation

of $\mathcal{A}_{CP}(B^+ \to \rho^0 K^+) = 0.150 \pm 0.019$ by LHCb recently [11]. In this case, one may argue that there are other possibilities that can produce *CP* violation, for example, a three-body rescattering including the third particle [12].

In QCDF, the decay amplitude of $B^- \to \rho^0 \pi^-$ is given by [15]

$$A(B^- \to \rho^0\pi^-) = \frac{G_F}{2} \sum_{p=u,c} \lambda_p^{(d)} \left\{ \left[\delta_{pu}(a_2 - \beta_2) - a_4^p - r_\chi^\rho a_6^p + \frac{3}{2}(a_7^p + a_9^p) + \frac{1}{2}(a_{10}^p + r_\chi^\rho a_8^p) - \beta_3^p - \beta_{3,\text{EW}}^p \right]_{\pi\rho} X^{(B^-\pi,\rho)} \right.$$
$$\left. + \left[\delta_{pu}(a_1 + \beta_2) + a_4^p - r_\chi^\pi a_6^p + a_{10}^p - r_\chi^\pi a_8^p + \beta_3^p + \beta_{3,\text{EW}}^p \right]_{\rho\pi} X^{(B^-\rho,\pi)} \right\}, \tag{2.5}$$

where $\lambda_p^{(d)} = V_{pb}V_{pd}^*$, the chiral factors $r_\chi^{\pi,\rho}$ are given by

$$r_\chi^\pi(\mu) = \frac{2m_\pi^2}{m_b(\mu)(m_u + m_d)(\mu)}, \qquad r_\chi^\rho(\mu) = \frac{2m_\rho}{m_b(\mu)} \frac{f_\rho^\perp(\mu)}{f_\rho}, \tag{2.6}$$

and the factorizable matrix elements read

$$X^{(B^-\pi,\rho)} = 2f_\rho m_B p_c F_1^{B\pi}(m_\rho^2),$$
$$X^{(B^-\rho,\pi)} = 2f_\pi m_B p_c A_0^{B\rho}(m_\pi^2), \tag{2.7}$$

with p_c being the c.m. momentum. Here, we have followed [16] for the definition of form factors. In Eq. (2.5), the flavor operators a_i^p have the expressions [15,17],

$$a_i^p(M_1M_2)$$
$$= c_i + \frac{c_{i\pm 1}}{N_c} + \frac{c_{i\pm 1}}{N_c} \frac{C_F\alpha_s}{4\pi} \left[V_i(M_2) + \frac{4\pi^2}{N_c} H_i(M_1M_2) \right]$$
$$+ P_i^p(M_2), \tag{2.8}$$

where $i = 1, \ldots, 10$, the upper (lower) signs apply when i is odd (even), c_i are the Wilson coefficients, $C_F = (N_c^2 - 1)/(2N_c)$ with $N_c = 3$. The quantities $V_i(M_2)$ account for vertex corrections, $H_i(M_1M_2)$ for hard spectator interactions with a hard gluon exchange between the emitted meson and the spectator quark of the B meson and $P_i(M_2)$ for penguin contractions. The order of the arguments of the $a_i^p(M_1M_2)$ and $\beta_i(M_1M_2)$ coefficients to be mentioned below is dictated by the subscript M_1M_2.

It is known that the leading-order $1/m_b$ predictions of QCDF encounter several major difficulties: (i) the predicted branching fractions for penguin-dominated $B \to PP, VP, VV$ decays are systematically below the measurements, (ii) the predicted rates for color-suppressed tree-dominated decays $B^0 \to \pi^0\pi^0, \rho^0\pi^0$ are too small, and (iii) direct CP asymmetries for $\bar{B}^0 \to K^-\pi^+, K^{*-}\pi^+, \pi^+\pi^-$, $B^- \to K^-\rho^0$ and $\bar{B}_s \to K^+\pi^-, \ldots$ etc., disagree with experiment in signs [4,18]. Hence, it is necessary to introduce $1/m_b$ power corrections to resolve above-mentioned difficulties. To solve the problems with (i) and (iii) in QCDF, power corrections to the penguin amplitudes are described by the penguin annihilation characterized by the parameters β_i^p [see Eq. (19) of Ref. [15] for the definition], for example, $\beta_{2,3}^p$ and $\beta_{3,\text{EW}}^p$ given in Eq. (2.5). Take the decay $\bar{B}^0 \to K^-\pi^+$ as an example. In the heavy quark limit, the

calculated branching fraction is too small by around 35% and the predicted CP violation is positive in sign (see, e.g., Table IV of Ref. [4]). However, the first evidence of direct CP asymmetry in B decays, namely, $\mathcal{A}_{CP}(\bar{B}^0 \to K^-\pi^+) = -0.133 \pm 0.031$ observed in 2004 [19] is negative. Power corrections from penguin annihilation solve the rate deficit and the sign problems at one stroke; see again Table IV of Ref. [4].

As pointed out in Refs. [4,18], sign flip of CP asymmetries in penguin-dominated due to the presence of power corrections from penguin annihilation will cause another CP puzzle: (iv) signs of $\mathcal{A}_{CP}$ in $B^- \to K^-\pi^0, K^-\eta, \pi^-\eta, \ldots$ will also get reversed in such a way that they disagree with experiment. It turns out that the difficulties with (ii) and (iv) can be resolved by invoking power corrections to hard spectator interactions. To see this, hard spectator interactions for $i = 1$–4, 9, 10 have the expression [15],

$$H_i(M_1M_2)$$
$$= \frac{if_B f_{M_1} f_{M_2}}{X^{(\bar{B}M_1,M_2)}} \frac{m_B}{\lambda_B} \int_0^1 dx$$
$$\times \int_0^1 dy \left(\frac{\Phi_{M_2}(x)\Phi_{M_1}(y)}{\bar{x}\,\bar{y}} + r_\chi^{M_1} \frac{\Phi_{M_2}(x)\Phi_{m_1}(y)}{\bar{x}y} \right), \tag{2.9}$$

with $\bar{x} = 1 - x$ and $\bar{y} = 1 - y$. Subleading $1/m_b$ power corrections stem from the twist-3 amplitude Φ_m. Hard spectator contributions to a_i are most prominent for a_2 as the Wilson coefficient c_1 is of order unity,

$$a_2(M_1M_2) = c_2 + \frac{c_1}{N_c}$$
$$+ \frac{c_1}{N_c} \frac{C_F\alpha_s}{4\pi} \left[V_2(M_2) + \frac{4\pi^2}{N_c} H_2(M_1M_2) \right]. \tag{2.10}$$

This explains why hard spectator interactions are helpful to account for the observed rates of $B^0 \to \pi^0\pi^0$ and $\rho^0\pi^0$.

In the QCD factorization approach, power corrections often involve end point divergences, for example, the second term in Eq. (2.9) is proportional to the end point divergence $X \equiv \int_0^1 dy/y$. We shall follow [17] to model the end point divergence in the penguin annihilation and hard spectator scattering diagrams as

$$X_A = \ln\left(\frac{m_B}{\Lambda_h}\right)(1 + \rho_A e^{i\phi_A}), \qquad X_H = \ln\left(\frac{m_B}{\Lambda_h}\right)(1 + \rho_H e^{i\phi_H}), \tag{2.11}$$

with Λ_h being a typical hadronic scale of 0.5 GeV. We add the superscripts "VP" and "PV" to distinguish penguin annihilation effects in $B \to VP$ and $B \to PV$ decays [15],

$$A_1^i \approx -A_2^i \approx 6\pi\alpha_s \left[3\left(X_A^{VP} - 4 + \frac{\pi^2}{3}\right) + r_\chi^V r_\chi^P ((X_A^{VP})^2 - 2X_A^{VP})\right],$$

$$A_3^i \approx 6\pi\alpha_s \left[-3r_\chi^V \left(\left(X_A^{VP}\right)^2 - 2X_A^{VP} + 4 - \frac{\pi^2}{3}\right) + r_\chi^P \left(\left(X_A^{VP}\right)^2 - 2X_A^{VP} + \frac{\pi^2}{3}\right)\right],$$

$$A_3^f \approx 6\pi\alpha_s [3r_\chi^V (2X_A^{VP} - 1)(2 - X_A^{VP}) - r_\chi^P (2(X_A^{VP})^2 - X_A^{VP})], \tag{2.12}$$

for $M_1 M_2 = VP$ and

$$A_1^i \approx -A_2^i \approx 6\pi\alpha_s \left[3\left(X_A^{PV} - 4 + \frac{\pi^2}{3}\right) + r_\chi^V r_\chi^P ((X_A^{PV})^2 - 2X_A^{PV})\right],$$

$$A_3^i \approx 6\pi\alpha_s \left[-3r_\chi^P \left(\left(X_A^{PV}\right)^2 - 2X_A^{PV} + 4 - \frac{\pi^2}{3}\right) + r_\chi^V \left(\left(X_A^{PV}\right)^2 - 2X_A^{PV} + \frac{\pi^2}{3}\right)\right],$$

$$A_3^f \approx 6\pi\alpha_s [-3r_\chi^P (2X_A^{PV} - 1)(2 - X_A^{PV}) + r_\chi^V (2(X_A^{PV})^2 - X_A^{PV})], \tag{2.13}$$

for $M_1 M_2 = PV$, where the superscripts "i" and "f" refer to gluon emission from the initial and final-state quarks, respectively, the subscripts 1 for the Dirac structure $(V - A) \otimes (V - A)$, 2 for $(V - A) \otimes (V + A)$ and 3 for $-2(S - P) \otimes (S + P)$.

The two unknown parameters ρ_A and ϕ_A were fitted to the data of $B \to PP, VP$ and PV decays. The values of ρ_A and ϕ_A are given, for example, in Table III of Ref. [4], where the results are very similar to the so-called "S4 scenario" presented in [15]. However, the measurement of the pure annihilation process $B_s^0 \to \pi^+\pi^-$ by CDF [20]

and LHCb [21] with the world average $\mathcal{B}(B_s \to \pi^+\pi^-) = (0.70 \pm 0.10) \times 10^{-6}$ [22] is much higher than the QCDF prediction of $(0.26^{+0.00+0.10}_{-0.00-0.09}) \times 10^{-6}$ [23]. Since this mode proceeds through the penguin-annihilation amplitudes A_1^i and A_2^i, it has been advocated that ρ_A's associated with the gluon emission from the initial and final-state quarks are different; that is, $\rho_A^i \neq \rho_A^f$ and that a much large ρ_A^i of order 3 can accommodate the data of $B_s^0 \to \pi^+\pi^-$ [24,25].

Nevertheless, a recent study of $B_s^0 \to \pi^+\pi^-$ in QCDF up to the NLL order given by [26]

$$A(B_s^0 \to \pi^+\pi^-) = \frac{G_F}{\sqrt{2}} \sum_{p=u,c} \lambda_p^{(s)} (if_B f_\pi^2) 4\pi\alpha_s \frac{C_F}{N_c^2}\left(T^{p,(0)} + \frac{\alpha_s}{4\pi}T^{p,(1)} + \cdots\right) \tag{2.14}$$

shows that the real part of $T^{c,(0)}$ is enhanced significantly, while the imaginary part gets considerable cancellation. More precisely, $T^{c,(0)} = -0.25 + 2.16i$ while $\alpha_s/(4\pi)T^{c,(1)} = -1.82 - 2.40i$ at $\mu = m_b$. Indeed, the weak annihilation diagram with the gluon emission from the initial-state quark is calculable to the leading power in $1/m_b$ expansion. It yields $(\rho_A^i, \phi_A^i)_{PP} = \{(0.97, -97°), (1.17, -97°), (1.34, -97°)\}$ for $\lambda_B = \{200, 350, 500\}$ MeV, respectively [26]. This implies that $(\rho_A^i)_{PP}$ is of order unity rather than 3. Moreover, the new measurement of another pure annihilation process $\mathcal{B}(B^0 \to K^+K^-) = (7.80 \pm 1.27 \pm 0.84) \times 10^{-8}$ by LHCb [27] is strongly disfavored with a large $(\rho_A^i)_{PP}$ as the predicted $\mathcal{B}(B^0 \to K^+K^-)$ will

be too large by a factor of $3 \sim 4$. Therefore, we will not distinguish between ρ_A^i and ρ_A^f.

For $B \to PV$ decays, (ρ_H, ϕ_H), $(\rho_A, \phi_A)_{VP}$ and $(\rho_A, \phi_A)_{PV}$ are treated as free parameters. In this work, we shall take

$$(\rho_A, \phi_A)_{PV} = (0.82, -37°), \quad (\rho_A, \phi_A)_{VP} = (0.68, -52°), \tag{2.15}$$

for calculations, where only the central values are listed here. The parameters $(\rho_A, \phi_A)_{PV}$ are inferred from $B \to \pi K^*$ decays, while $(\rho_A, \phi_A)_{VP}$ from $B \to \rho K$ ones. In the

TABLE I.   The branching fraction and CP asymmetry of $B^- \to \rho^0\pi^-$ within the QCDF approach. Experimental data are taken from [22]. The theoretical errors correspond to the uncertainties due to the variation of (i) Gegenbauer moments, decay constants, form factors, the strange quark mass, and (ii) $\rho_{A,H}$, $\phi_{A,H}$, respectively. In (ii), we assign an error of ± 0.4 to ρ and $\pm 4°$ to ϕ.

$\mathcal{B}(10^{-6})$	$\mathcal{A}_{CP}(\%)$	Comments
8.3 ± 1.2	0.7 ± 1.9	Experiment
$8.3^{+1.9+0.0}_{-0.9-0.0}$	$6.6^{+0.5+0.0}_{-0.8-0.0}$	(1) Heavy quark limit
$8.5^{+1.9+0.2}_{-0.9-0.2}$	$-11.8^{+0.9+3.6}_{-0.7-3.9}$	(2) $\rho_H = 0$ and $\phi_H = 0$ with ρ_A and ϕ_A given by Eq. (2.15)
$7.5^{+1.5+0.1}_{-0.7-0.2}$	$15.6^{+1.3+1.2}_{-1.1-1.5}$	(3) $\rho_H = 3.15$, $\phi_H = -113°$, $\rho_A = 0$, $\phi_A = 0$
$7.7^{+1.5+0.2}_{-0.7-0.2}$	$-0.5^{+3.9+3.5}_{-2.6-3.8}$	(4) $\rho_H = 3.15$, $\phi_H = -113°$, ρ_A and ϕ_A given by Eq. (2.15)

PP sector, we have $(\rho_A, \phi_A)_{PP} = (1.05, -40°)$. For CP violation in the VP sector, we find

$$\mathcal{A}_{CP}(\bar{B}^0 \to K^{*-}\pi^+) = -(17.3^{+0.9+3.7}_{-1.3+3.2})\%,$$
$$\mathcal{A}_{CP}(B^- \to \rho^0 K^-) = (28.7^{+21.5+2.5}_{-20.5-3.3})\%, \qquad (2.16)$$

while the experimental measurements are -0.271 ± 0.044 [13] and 0.150 ± 0.019 [11], respectively.

As noticed in passing, it is necessary to introduce the power corrections from hard spectator interactions characterized by ρ_H and ϕ_H to not only account for the rate deficit of the color-suppressed tree-dominated modes $B^0 \to \pi^0\pi^0$ and $\rho^0\pi^0$ but also resolve the CP puzzles with some of the penguin-dominated modes such as $B^- \to K^-\eta$, $B^0 \to K^{*0}\eta$ and $B^- \to K^-\pi^0$, where the last one is related to the so-called $\Delta\mathcal{A}_{K\pi}$ puzzle with $\Delta\mathcal{A}_{K\pi} \equiv \mathcal{A}_{CP}(B^- \to K^-\pi^0) - \mathcal{A}_{CP}(\bar{B}^0 \to K^-\pi^+)$. In the absence of hard spectator interactions, CP asymmetries of $B^- \to K^-\eta$, $B^0 \to K^{*0}\eta$, $B^- \to K^-\pi^0$ and $\Delta\mathcal{A}_{K\pi}$ are calculated to be 0.045, 0.010, -0.035 and 0.022, respectively, while the corresponding measured values are -0.37 ± 0.08, 0.19 ± 0.05, 0.030 ± 0.013 and 0.115 ± 0.014 [22]. One needs hard spectator interactions to flip the signs of $\mathcal{A}_{CP}(B^- \to K^-\eta)$, $\mathcal{A}_{CP}(B^- \to K^-\pi^0)$ and enhance $\mathcal{A}_{CP}(B^0 \to K^{*0}\eta)$. Specifically, we shall use

$$(\rho_H, \phi_H)_{PV,VP} = (3.15, -113°),$$
$$(\rho_H, \phi_H)_{PP} = (4.0, -70°). \qquad (2.17)$$

to accommodate the above-mentioned data. Notice that ρ_H is much larger than ρ_A.

We are now ready to compute the branching fraction and CP asymmetry for $B^- \to \rho^0\pi^-$; see Table I. In the heavy quark limit, its CP asymmetry is positive with a magnitude of order 0.07 . We then turn on power corrections induced from penguin annihilation. It is clear that the sign of $\mathcal{A}_{CP}(\rho^0\pi^-)$ is flipped, and in the meantime, its magnitude is enhanced. We next switch on $1/m_b$ corrections from hard spectator interactions and turn off ρ_A and ϕ_A. It is evident that $\mathcal{A}_{CP}(\rho^0\pi^-)$ will be enhanced from $\mathcal{O}(0.07)$ to $\mathcal{O}(0.16)$ in the presence of hard spectator effects alone. If the heavy

quark limit of $\mathcal{A}_{CP}(\rho^0\pi^-)$ is considered as a benchmark, hard spectator interactions will push it up further, whereas penguin annihilation will pull it to the opposite direction. Therefore, the nearly vanishing $\mathcal{A}_{CP}(\rho^0\pi^-)$ arises from two $1/m_b$ power corrections which contribute destructively.

At the first sight, it appears from Table I that the calculated branching fraction of order 7.7×10^{-6} is slightly smaller than the experimental value of $(8.3 \pm 1.2) \times 10^{-6}$ [22]. In the particle data group (PDG) [22], the branching fraction of $B^- \to \rho^0\pi^-$ is extracted from the measurement of $B^- \to \rho^0\pi^- \to \pi^+\pi^-\pi^-$ through the factorization relation,

$$\mathcal{B}(B^- \to \rho^0\pi^- \to \pi^+\pi^-\pi^-)$$
$$= \mathcal{B}(B^- \to \rho^0\pi^-)\mathcal{B}(\rho^0 \to \pi^+\pi^-)$$
$$= \mathcal{B}(B^- \to \rho^0\pi^-), \qquad (2.18)$$

which is valid only in the narrow width approximation (NWA). Since $\rho(770)$ is broad with a width of 149 MeV, it is necessary to consider the finite-width effect. The η_R parameters for various resonances produced in three-body B decays have been evaluated in [28,29],

$$\mathcal{B}(B \to RP) = \eta_R \mathcal{B}(B \to RP)_{\text{NWA}}$$
$$= \eta_R \frac{\mathcal{B}(B \to RP_3 \to P_1P_2P_3)_{\text{expt}}}{\mathcal{B}(R \to P_1P_2)_{\text{expt}}}. \qquad (2.19)$$

The parameter η_ρ depends on the line shape of the $\rho(770)$ meson, and it has been calculated in QCDF [28,29]. It was found $\eta_\rho^{GS} = 0.93$ in the Gounaris-Sakurai (GS) model [30] to be discussed below for the ρ line shape adapted by both LHCb [1,2] and *BABAR* [31] in the analysis of $B^\pm \to \pi^+\pi^-\pi^\pm$ decays. It follows that the PDG value of $\mathcal{B}(B^- \to \rho\pi^-) = (8.3 \pm 1.2) \times 10^{-6}$ should be corrected to $(7.7 \pm 1.1) \times 10^{-6}$ after including finite-width effects.

III. $B^\pm \to \sigma\pi^\pm$ DECAYS

The decay $B^- \to \sigma/f_0(500)\pi^-$ has been studied in Ref. [32]. Its decay amplitude has a similar expression as $B^- \to f_0(980)\pi^-$ and reads

$$A(B^- \to \sigma\pi^-) = \frac{G_F}{\sqrt{2}} \sum_{p=u,c} \lambda_p^{(d)} \left\{ [a_1 \delta_{pu} + a_4^p + a_{10}^p - (a_6^p + a_8^p) r_\chi^\pi]_{\sigma\pi} X^{(B\sigma,\pi)} \right.$$

$$+ \left[a_2 \delta_{pu} + 2(a_3^p + a_5^p) + \frac{1}{2}(a_7^p + a_9^p) + a_4^p - \frac{1}{2} a_{10}^p - \left(a_6^p - \frac{1}{2} a_8^p \right) \bar{r}_\chi^\sigma \right]_{\pi\sigma} \bar{X}^{(B\pi,\sigma)}$$

$$\left. - f_B f_\pi \bar{f}_\sigma^u [\delta_{pu} b_2(\pi\sigma) + b_3(\pi\sigma) + b_{3,\text{EW}}(\pi\sigma) + (\pi\sigma \to \sigma\pi)] \right\}, \tag{3.1}$$

where the factorizable matrix elements are given by

$$X^{(B\sigma,\pi)} = -f_\pi F_0^{B\sigma^u}(m_\pi^2)(m_B^2 - m_\sigma^2),$$
$$\bar{X}^{(B\pi,\sigma)} = \bar{f}_\sigma^u F_0^{B\pi}(m_\sigma^2)(m_B^2 - m_\pi^2), \tag{3.2}$$

with $\bar{r}_\chi^\sigma(\mu) = 2m_\sigma/m_b(\mu)$. The superscript u in the scalar decay constant $\bar{f}_\sigma^u$ and the form factor $F^{B\sigma^u}$ refers to the u quark component of the σ. The scale-dependent scalar decay constant is defined by $\langle \sigma | \bar{u}u | 0 \rangle = m_\sigma \bar{f}_\sigma^u$ [33]. We follow [32] to take $\bar{f}_\sigma^u = 350$ MeV at $\mu = 1$ GeV and $F_0^{B\sigma^u}(0) = 0.25$.

Numerical values of the flavor operators $a_i^p(\sigma\pi)$ and $a_i^p(\pi\sigma)$ at the scale $\mu = m_b(m_b)$ and penguin annihilation characterized by the parameter β^p are shown in Table IV of Ref. [32]. It follows that the flavor operators $a_i^p(\sigma\pi)$ and $a_i^p(\pi\sigma)$ are very different except for $a_{6,8}^p$ as the former do not receive factorizable contributions. As a consequence, $a_1(\sigma\pi) \approx 1 \gg a_1(\pi\sigma)$.

Numerically, we obtain

$$\mathcal{B}(B^- \to \sigma\pi^-) = (5.15_{-1.16-1.29}^{+1.31+0.86}) \times 10^{-6},$$
$$\mathcal{A}_{CP}(B^- \to \sigma\pi^-) = (15.10_{-0.30-11.38}^{+0.31+8.36})\%, \tag{3.3}$$

where use of the Wolfenstein parameters updated with $A = 0.8132$, $\lambda = 0.22500$, $\bar{\rho} = 0.1566$, and $\bar{\eta} = 0.3475$ [34] has been made. Theoretical uncertainties come from (i) the Gegenbauer moments $B_{1,3}$, the scalar meson decay constants, the heavy-to-light form factors, and the strange quark mass, and (ii) the power corrections due to weak annihilation and hard spectator interactions, respectively. The calculated CP asymmetry agrees well with the LHCb measurement analyzed in the isobar model [1,2],

$$\mathcal{A}_{CP}(B^- \to \sigma\pi^-) = (16.0 \pm 1.7 \pm 2.2)\%. \tag{3.4}$$

IV. INTERFERENCE BETWEEN $\rho(770)$ AND $\sigma(500)$ RESONANCES

In this section, we consider the three-body $B^- \to \pi^-\pi^+\pi^-$ decays mediated by the $\rho(770)$ and $\sigma(500)$ resonances and study their interference. For the three-body decay amplitude $A_-^\rho \equiv A(B^- \to \rho^0(770)\pi^- \to \pi^-(p_1)\pi^+(p_2)\pi^-(p_3))$, factorization leads to the expression [35],

$$A_-^\rho = -g^{\rho \to \pi^+\pi^-} F(s_{12}, m_\rho) T_\rho^{\text{GS}}(s_{12}) 2q \cos\theta \tilde{A}(B^- \to \rho\pi^-)$$
$$+ (s_{12} \leftrightarrow s_{23}), \tag{4.1}$$

where q given by

$$q = |\vec{p}_1| = |\vec{p}_2| = \frac{1}{2}\sqrt{s_{12} - 4m_\pi^2}, \tag{4.2}$$

is the momenta of $\pi^-(p_1)$ and $\pi^+(p_2)$ in the rest frame of the ρ with the invariant mass $m_{12} = \sqrt{s_{12}}$, $\tilde{A}(B^- \to \rho\pi^-)$ has the same expression as $A(B^- \to \rho\pi^-)$ given in Eq. (2.5) except for the replacement of $X^{(B^-\pi,\rho)}$ and $X^{(B^-\rho,\pi)}$ by

$$\tilde{X}^{(B^-\pi,\rho)} = 2f_\rho m_B \tilde{p}_c F_1^{B\pi}(s_{12}),$$

$$\tilde{X}^{(B^-\rho,\pi)} = 2f_\pi m_B \tilde{p}_c \left[A_0^{B\rho}(m_\pi^2) \right.$$
$$\left. + \frac{1}{2m_\rho}\left(m_B - m_\rho - \frac{m_B^2 - s_{12}}{m_B + m_\rho} \right) A_2^{B\rho}(m_\pi^2) \right], \tag{4.3}$$

respectively, with[2]

$$\tilde{p}_c = \left(\frac{(m_B^2 - m_\pi^2 - s_{12})^2 - 4s_{12}m_\pi^2}{4m_B^2} \right)^{1/2}, \tag{4.4}$$

being the c.m. momentum of $\pi^-(p_3)$ and the $\rho(m_{12})$ in the B rest frame. It is easily seen that when $s_{12} \to m_\rho^2$, $\tilde{A}(B^- \to \rho\pi^-)$ is reduced to the QCDF amplitude $A(B^- \to \rho\pi^-)$ given by Eq. (2.5).

When ρ is off the mass shell, especially when s_{12} is approaching the upper bound of $(m_B - m_\pi)^2$, it is necessary to account for the off shell effect. For this purpose, we shall follow [36] to introduce a form factor $F(s, m_R)$ parametrized as

$$F(s, m_R) = \left(\frac{\Lambda^2 + m_R^2}{\Lambda^2 + s} \right)^n, \tag{4.5}$$

with the cutoff Λ not far from the resonance,

---

[2]The momentum $|\vec{p}_3|$ is related to $\tilde{p}_c$ by the relation $|\vec{p}_3| = (m_B/m_{12})\tilde{p}_c$.

$$\Lambda = m_R + \beta\Lambda_{\mathrm{QCD}}, \tag{4.6}$$

where the parameter β is expected to be of order unity. We shall use $n = 1$, $\Lambda_{\mathrm{QCD}} = 250$ MeV and $\beta = 1.0 \pm 0.2$ in subsequent calculations.

In Eq. (4.1), T_ρ^{GS} is a description of the broad $\rho(770)$ resonance in the Gounaris-Sakurai (GS) model [30]. It was employed by both *BABAR* [31] and LHCb [1,2] Collaborations in their analyses of the $\rho(770)$ resonance in the $B^- \to \pi^- \pi^+ \pi^-$ decay. The GS line shape for $\rho(770)$ is given by

$$T_\rho^{\mathrm{GS}}(s) = \frac{1 + D\Gamma_\rho^0/m_\rho}{s - m_\rho^2 - f(s) + im_\rho\Gamma_\rho(s)}, \tag{4.7}$$

where

$$\Gamma_\rho(s) = \Gamma_\rho^0\left(\frac{q}{q_0}\right)^3 \frac{m_\rho}{\sqrt{s}} \frac{X_1^2(q)}{X_1^2(q_0)}, \tag{4.8}$$

with Γ_ρ^0 being the nominal total ρ width with $\Gamma_\rho^0 = \Gamma_\rho(m_\rho^2)$ and the Blatt-Weisskopf barrier factor given by $X_1^2(z) = 1/[(zr_{\mathrm{BW}})^2 + 1]$ and $r_{\mathrm{BW}} \approx 4.0$ GeV^{-1}. The quantity q_0 is the value of q when m_{12} is equal to the pole mass m_ρ. In this model, the real part of the pion-pion scattering amplitude with an intermediate ρ exchange calculated from the dispersion relation is taken into account by the $f(s)$ term in the propagator of $T_\rho^{\mathrm{GS}}(s)$. Explicitly,

$$f(s) = \Gamma_\rho^0 \frac{m_\rho^2}{q_0^3}\left[q^2[h(\sqrt{s}) - h(m_\rho)] + (m_\rho^2 - s)q_0^2\frac{dh}{ds}\bigg|_{m_\rho}\right], \tag{4.9}$$

and

$$h(s) = \frac{2}{\pi}\frac{q}{\sqrt{s}}\ln\left(\frac{\sqrt{s} + 2q}{2m_\pi}\right),$$
$$\frac{dh}{ds}\bigg|_{m_\rho} = h(m_\rho)\left[\frac{1}{8q_0^2} - \frac{1}{2m_\rho^2}\right] + \frac{1}{2\pi m_\rho^2}. \tag{4.10}$$

The constant parameter D is given by

$$D = \frac{3}{\pi}\frac{m_\pi^2}{q_0^2}\ln\left(\frac{m_\rho + 2q_0}{2m_\pi}\right) + \frac{m_\rho}{2\pi q_0} - \frac{m_\pi^2 m_\rho}{\pi q_0^3}. \tag{4.11}$$

Likewise, for the decay amplitude $A_-^\sigma \equiv A(B^- \to \sigma\pi^- \to \pi^+\pi^-\pi^-)$, factorization leads to [35]

$$A_-^\sigma = g^{\sigma\to\pi^+\pi^-}F(s_{12}, m_\sigma)T_\sigma(s_{12})\tilde{A}(B^- \to \sigma\pi^-)$$
$$+ (s_{12} \leftrightarrow s_{23}), \tag{4.12}$$

where $\tilde{A}(B^- \to \sigma\pi^-)$ has the same expression as $A(B^- \to \sigma\pi^-)$ given in Eq. (3.1) with the replacement,

$$X^{(B\sigma,\pi)} \to \tilde{X}^{(B\sigma,\pi)} = -f_\pi(m_B^2 - s_{12})F_0^{B\sigma^u}(m_\pi^2),$$
$$X^{(B\pi,\sigma)} \to \tilde{X}^{(B\pi,\sigma)} = \bar{f}_\sigma^u(m_B^2 - m_\pi^2)F_0^{B\pi}(s_{12}). \tag{4.13}$$

For the σ line shape, we follow the LHCb Collaboration [2] to use the simple pole description,

$$T_\sigma(s) = \frac{1}{s - s_\sigma} = \frac{1}{s - m_\sigma^2 + \Gamma_\sigma^2(s)/4 + im_\sigma\Gamma_\sigma(s)}, \tag{4.14}$$

with

$$\Gamma_\sigma(s) = \Gamma_\sigma^0\left(\frac{q}{q_0}\right)\frac{m_\sigma}{\sqrt{s}}, \tag{4.15}$$

and

$$\sqrt{s_\sigma} = m_\sigma - i\Gamma_\sigma/2 = (563 \pm 10) - i(350 \pm 13) \text{ MeV}, \tag{4.16}$$

obtained from the isobar description of the $\pi^+\pi^-$ S-wave to fit the $B^- \to \pi^-\pi^+\pi^-$ decay data [2].

Strong coupling constants $g^{\rho\to\pi^+\pi^+}$ in Eq. (4.1) and $g^{\sigma\to\pi^+\pi^-}$ in Eq. (4.12) are determined from the measured widths through the relations,

$$\Gamma_{S\to P_1 P_2} = \frac{p_c}{8\pi m_S^2}g_{S\to P_1 P_2}^2, \qquad \Gamma_{V\to P_1 P_2} = \frac{p_c^3}{6\pi m_V^2}g_{V\to P_1 P_2}^2. \tag{4.17}$$

Numerically,

$$|g^{\rho\to\pi^+\pi^+}| = 6.00, \quad |g^{\sigma\to\pi^+\pi^-}| = 3.90 \text{ GeV}. \tag{4.18}$$

In the LHCb experiment, CP violation induced by the interference between P- and S-waves is measured in the low-$m_{\pi^+\pi^-}$ region, where the data are separated by the sign of $\cos\theta$ or $\cos\theta_{\mathrm{hel}}$; see Fig. 1. The $\cos\theta$ term can be expressed as a function of s_{12} and s_{23},

$$\cos\theta = a(s_{12})s_{23} + b(s_{12}), \tag{4.19}$$

with [3]

$$a(s) = \frac{1}{(s - 4m_\pi^2)^{1/2}\left(\frac{(m_B^2 - m_\pi^2 - s)^2}{4s} - m_\pi^2\right)^{1/2}},$$

$$b(s) = -\frac{m_B^2 + 3m_\pi^2 - s}{2(s - 4m_\pi^2)^{1/2}\left(\frac{(m_B^2 - m_\pi^2 - s)^2}{4s} - m_\pi^2\right)^{1/2}}. \tag{4.20}$$
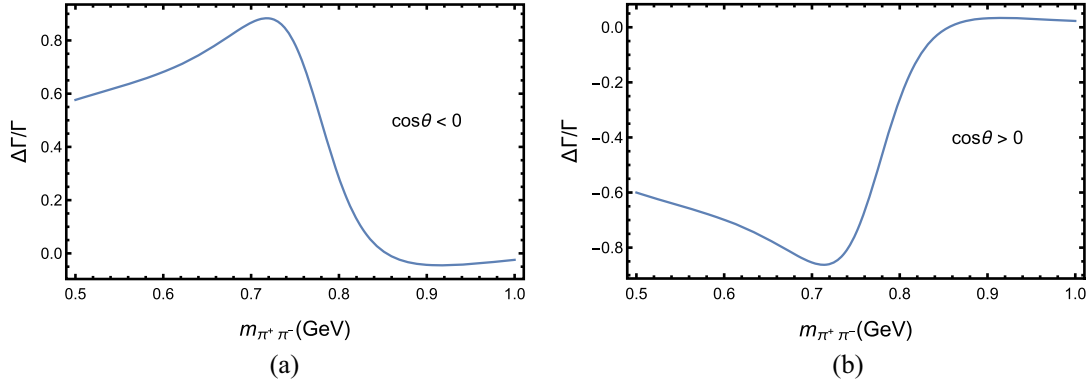
FIG. 3. Rate asymmetries $\Delta\Gamma$ in units of $\Gamma = 1/\tau(B^\pm)$ for $B^\pm \to \pi^\pm\pi^+\pi^-$ in the low-$m_{\pi^+\pi^-}$ region induced by the $\rho(770)$ and σ interference for (a) $\cos\theta < 0$ ($\cos\theta_{\rm hel} > 0$) and (b) $\cos\theta > 0$ ($\cos\theta_{\rm hel} < 0$). The relative phases between $A^\sigma_\pm$ and $A^\rho_\pm$ are set to zero.

Note that the cosine of the angle θ with the values -1, 0, and 1 corresponds to $(s_{23})_{\rm min} = -(1+b)/a$, $s_{23} = -b/a$, and $(s_{23})_{\rm max} = (1-b)/a$, respectively.

The three-body decay rates involving ρ, σ and their interference in the negative and positive $\cos\theta$ regions are given by

$$\Gamma^{\rho-\sigma}_\pm(s_{12})^{(\cos\theta<0)} = \frac{1}{(2\pi)^3 32 m_B^3} \frac{G_F^2}{2} \frac{1}{2} \int_{(s_{23})_{\rm min}}^{-b/a} (|A^\rho_\pm|^2 + |A^\sigma_\pm|^2 + 2[\mathrm{Re}(A^\rho_\pm)\mathrm{Re}(A^\sigma_\pm) + \mathrm{Im}(A^\rho_\pm)\mathrm{Im}(A^\sigma_\pm)])ds_{23} \quad \text{for } \cos\theta < 0,$$

$$\Gamma^{\rho-\sigma}_\pm(s_{12})^{(\cos\theta>0)} = \frac{1}{(2\pi)^3 32 m_B^3} \frac{G_F^2}{2} \frac{1}{2} \int_{-b/a}^{(s_{23})_{\rm max}} (|A^\rho_\pm|^2 + |A^\sigma_\pm|^2 + 2[\mathrm{Re}(A^\rho_\pm)\mathrm{Re}(A^\sigma_\pm) + \mathrm{Im}(A^\rho_\pm)\mathrm{Im}(A^\sigma_\pm)])ds_{23} \quad \text{for } \cos\theta > 0,$$

$$(4.21)$$

where the identical particle effect has been taken care of by the factor of $1/2$, and the amplitudes $A^\rho_\pm$ and $A^\sigma_\pm$ are given by Eqs. (4.1) and (4.12), respectively. In the above equation, the $\rho(770)$ and σ interference is depicted by the terms $[\mathrm{Re}(A^\rho_\pm)\mathrm{Re}(A^\sigma_\pm) + \mathrm{Im}(A^\rho_\pm)\mathrm{Im}(A^\sigma_\pm)]$. The rate difference $\Delta\Gamma^{\rho-\sigma} \equiv \Gamma^{\rho-\sigma}_- - \Gamma^{\rho-\sigma}_+$ due to the $\rho(770)$ and σ interference is shown in Figs. 3(a) and 3(b) for $\cos\theta < 0$ (or $\cos\theta_{\rm hel} > 0$) and $\cos\theta > 0$ (or $\cos\theta_{\rm hel} < 0$), respectively. It is obvious that they do not resemble the data displayed in Fig. 1 at all. For example, the shapes are quite different from that of the data and the characteristic feature of $(s_{12} - m_\rho^2)\cos\theta$ is absent.[3]

This above-mentioned difficulty is resolved by noticing a nontrivial global phase difference between ρ and σ. Indeed, the phase ϕ_- (ϕ_+) of the $A^\sigma_\mp$ relative to $A^\rho_\mp$ in B^- (B^+) decays has been measured by LHCb to be

$$\phi_-^{\rm expt} = 115 \pm 2 \pm 14, \qquad \phi_+^{\rm expt} = 179 \pm 1 \pm 95, \quad (4.22)$$

in units of degrees (see Table I of [1]). Assigning the phases ϕ_- and ϕ_+ to the amplitudes A^σ_- and A^σ_+, respectively, we

find the observed interference pattern in Figs. 1(a) and 1(b) for $\cos\theta < 0$ and $\cos\theta > 0$, respectively, can be properly reproduced in Figs. 4(a) and 4(b), respectively, with

$$\phi_- = 115°, \qquad \phi_+ = 127°. \quad (4.23)$$

Since the measured phase ϕ_+ has a large uncertainty, we have fixed ϕ_- to its central value 115° and varied ϕ_+ within the experimental allowed region. We find that the phase ϕ_+ is in the vicinity of 127°. However, it is not clear to us what the dynamical origin of the phase difference is.

Thus far, we have neglected *CP*-violating contributions from ρ and σ to rate asymmetries, namely, the first two terms in Eq. (1.3). Figures 5(a) and 5(b) show the rate asymmetries of $B^\pm \to \sigma\pi^\pm \to \pi^+\pi^-\pi^\pm$ and $B^\pm \to \rho^0\pi^\pm \to \pi^+\pi^-\pi^\pm$, respectively, as a function of low-$m_{\pi^+\pi^-}$ between 0.5 and 1.0 GeV for either $\cos\theta < 0$ or $\cos\theta > 0$,[4] corresponding to $\mathcal{A}_{CP}(B^\pm \to \sigma\pi^\pm) = 0.15$ [see Eq. (3.3)] and $\mathcal{A}_{CP}(B^\pm \to \rho^0\pi^\pm) = -0.005$ (see Table I). After adding the rate asymmetries from ρ and σ from Figs. 5(a) and 5(b), respectively, to both Figs. 4(a) and 4(b), we finally get Figs. 4(c) and 4(d) for $\cos\theta < 0$ and $\cos\theta > 0$,

---

[3]In our previous work [35], Figs. 5(a) and 5(b) were obtained by setting β's, the parameters describing weak annihilation, to be zero. The relative phases between $A^\sigma_\pm$ and $A^\rho_\pm$ were also not taken into account.

[4]They do not change sign when the cosine varies from -1 to $+1$ as $|A^\rho_\pm|^2$ are proportional to $\cos\theta^2$, while $|A^\sigma_\pm|^2$ are θ independent.

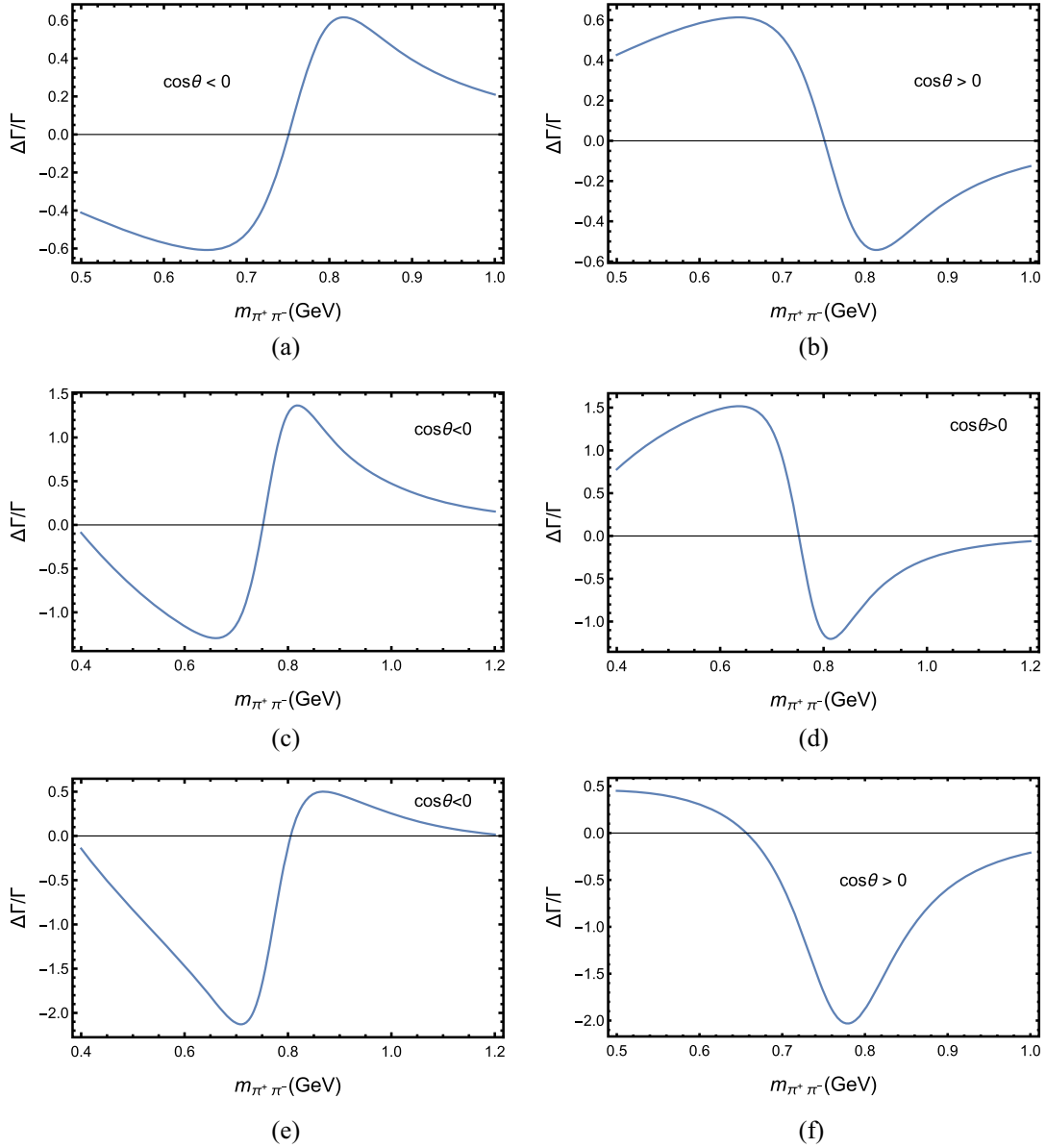FIG. 4. The rate asymmetry $\Delta\Gamma$ in units of $\Gamma = 1/\tau(B^\pm)$ for $B^\pm \to \pi^\pm\pi^+\pi^-$ in the low-$m_{\pi^+\pi^-}$ region induced by the interference between $\rho(770)$ and the σ meson for (a) $\cos\theta < 0$ or $\cos\theta_{\rm hel} > 0$ and (b) $\cos\theta > 0$ or $\cos\theta_{\rm hel} < 0$. Rate asymmetries of $\rho(770)$ and σ are added to (a) and (b) and shown in (c) and (d), respectively. The phases of $A_\pm^\sigma$ relative to $A_\pm^\rho$ are given by Eq. (4.23).

respectively. By comparing them with Fig. 1, we see that the resultant rate asymmetries agree well with the experimental observation, namely the peak height and the bottom depth are similar in magnitude with the former slightly larger. The curve below $m_{\pi^+\pi^-} \sim 700$ MeV in Fig. 4(d) becomes flat owing to the contribution from the σ resonance at lower $m_{\pi^+\pi^-}$.

Two remarks are in order. (i) The real part of the GS line shape is proportional to $s - m_\rho^2 - f(s)$ rather than $s - m_\rho^2$. Nevertheless, we find that the contribution from $f(s)$ is numerically small and can be neglected. (ii) Rate asymmetries do not vanish exactly at $m_{\pi^+\pi^-} = m_\rho$ due to other contributions such as the real part of the line shape; see Eq. (1.3).

If the CP asymmetry of the quasi-two-body decay $B^\pm \to \rho^0\pi^\pm$ is not neligible, what will the rate asymmetry look like? For an illustration, we shall take the case (ii) in Table I as an example, namely, $\mathcal{A}_{CP}(B^\pm \to \rho^0\pi^\pm) = -0.12$ obtained in QCDF by setting both ρ_H and ϕ_H to zero. $\Delta\Gamma/\Gamma$ due to the ρ resonance is now shown in Fig. 5(c). The rate asymmetries due to the $\rho - \sigma$ interference are very similar to that of Figs. 4(a) and 4(b) for $\cos\theta < 0$ and $\cos\theta > 0$, respectively. Adding contributions from Figs. 5(a) and 5(c) to Figs. 4(a) and 4(b) yield the final rate asymmetries in Figs. 4(e) and 4(f) for $\cos\theta < 0$ and $\cos\theta > 0$, respectively. It is obvious that CP asymmetries are pushed downward owing to the negative CP violation in
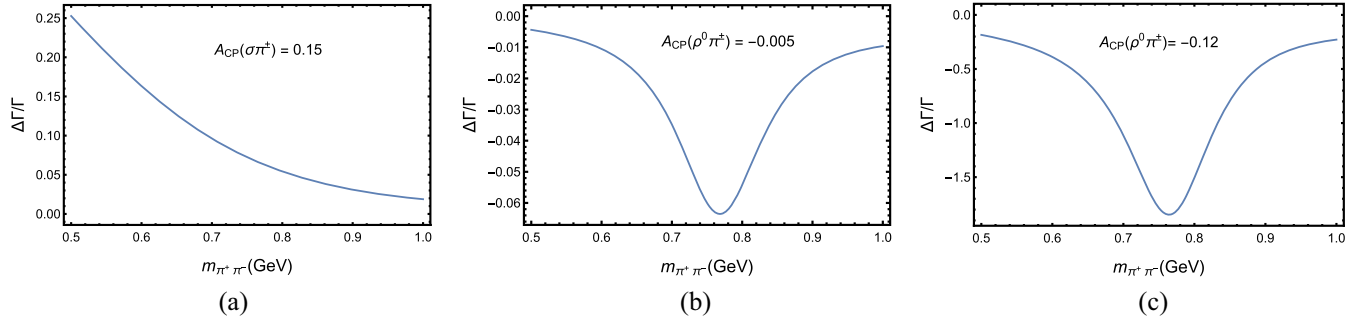
FIG. 5.   Rate asymmetries $\Delta\Gamma$ in units of $\Gamma = 1/\tau(B^\pm)$ for $B^\pm \to \pi^\pm\pi^+\pi^-$ in the low-$m_{\pi^+\pi^-}$ region induced by the σ meson (a) and the $\rho(770)$ [(b) and (c)] for either $\cos\theta < 0$ or $\cos\theta > 0$. (a) corresponds to $\mathcal{A}_{CP}(B^\pm \to \sigma\pi^\pm) = 0.15$, (b) to $\mathcal{A}_{CP}(B^\pm \to \rho^0\pi^\pm) = -0.005$, and (c) to $\mathcal{A}_{CP}(B^\pm \to \rho^0\pi^\pm) = -0.12$.

$B^\pm \to \rho^0\pi^\pm$. Evidently, the patterns exhibited in Figs. 4(e) and 4(f) are not consistent with the data. Indeed, rate asymmetries do not cancel when integrating over the angle. We thus conclude that the experimental observation of the interference pattern between *P*- and *S*-waves in the low-$m_{\pi^+\pi^-}$ region between 0.5 and 1.0 GeV is consistent with a nearly vanishing *CP* violation in $B^\pm \to \rho^0\pi^\pm$.

For the interference between *P*- and *S*-waves, we have thus far focused on the *S*-wave contribution from the σ resonance. In principle, the interference of $\rho(770)$ with $f_0(980)$ and the nonresonant component as considered in [3] is also allowed. Since the quasi-two-body decay $B^+ \to f_0(980)\pi^+$ is quite suppressed [37], the $f_0(980)$ fraction should be less than 1% (see, e.g., Table VI of Ref. [35]), much smaller than the σ fraction of 25% in the isobar model. The nonresonant contribution was not specified in the LHCb analysis, though it has been studied in the earlier *BABAR* measurement [31]. Therefore, in this work, we will not consider the interference of $\rho(770)$ with $f_0(980)$ and the nonresonant background.

V. CONCLUSIONS

The decay amplitudes of $B^\pm \to \pi^+\pi^-\pi^\pm$ in the Dalitz plot analyzed by the LHCb indicate that *CP* asymmetry for the dominant quasi-two-body decay $B^\pm \to \rho(770)^0\pi^\pm$ was found to be consistent with zero in all three approaches for the *S*-wave component and that *CP*-violation effects related to the interference between the $\rho(770)^0$ resonance and the *S*-wave were clearly observed. We show that the nearly vanishing *CP* violation in $B^\pm \to \rho^0\pi^\pm$ is understandable in the framework of QCD factorization. There exist two $1/m_b$ power corrections, one from penguin annihilations and the other from hard spectator interactions. In the heavy quark

limit, $\mathcal{A}_{CP}(B^\pm \to \rho^0\pi^\pm)$ turns out to be positive. Hard spectator interactions will push it up further, whereas penguin annihilation will pull it to the opposite direction. These two power corrections contribute destructively to $\mathcal{A}_{CP}(B^\pm \to \rho^0\pi^\pm)$ to render it consistent with zero, in contrast to the non-negligible *CP* asymmetry predicted in most of the existing models.

We next show that the measured interference pattern between the ρ and *S*-wave contributions in the low $m_{\pi^+\pi^-}$ region separated by the sign of value of $\cos\theta$ can be explained in terms of the smallness of $\mathcal{A}_{CP}(B^+ \to \rho^0\pi^+)$ and the interference between $\rho(770)$ and $\sigma/f_0(500)$. There are two key ingredients needed for producing the observed interference curve: one is the global phase difference between $\rho(770)$ and σ contributions in B^- and B^+ decays, which has been measured by LHCb. The other is the long-distance strong phase arising from the line shape of the intermediate resonance. In particular, the real and imaginary parts of the Breit-Wigner propagator with the ρ resonance are proportional to $s - m_\rho^2$ and $m_\rho\Gamma_\rho$, respectively. The characteristic feature of the interference pattern, namely, *CP* asymmetry is proportional to $(s - m_\rho^2)\cos\theta$, is thus accounted for, as shown in Figs. 4(c) and 4(d). If *CP* asymmetry in $B^\pm \to \rho^0\pi^\pm$ is not negligible as predicted in many existing models, the observed interference pattern will be destroyed; see, e.g., Figs. 4(e) and 4(f). This again implies a nearly vanishing *CP* violation in $B^\pm \to \rho^0\pi^\pm$.

[1] R. Aaij *et al.* (LHCb Collaboration), Observation of Several Sources of *CP* Violation in $B^+ \to \pi^+\pi^+\pi^-$ Decays, Phys. Rev. Lett. **124,** 031801 (2020).

[2] R. Aaij *et al.* (LHCb Collaboration), Amplitude analysis of the $B^+ \to \pi^+\pi^+\pi^-$ decay, Phys. Rev. D **101,** 012006 (2020).

[3] J. H. Alvarenga Nogueira, I. Bediaga, A. B. R. Cavalcante, T. Frederico, and O. Lourenmo, *CP* violation: Dalitz interference, *CPT*, and final state interactions, Phys. Rev. D **92,** 054010 (2015).

[4] H. Y. Cheng and C. K. Chua, Revisiting charmless hadronic $B_{u,d}$ decays in QCD factorization, Phys. Rev. D **80,** 114008 (2009).

[5] J. Sun, Q. Chang, X. Hu, and Y. Yang, Constraints on hard spectator scattering and annihilation corrections in $B_{u,d} \to PV$ decays within QCD factorization, Phys. Lett. B **743,** 444 (2015).

[6] Y. Li, A. Ma, W. Wang, and Z. Xiao, Quasi-two-body decays $B_{(s)} \to P\rho \to P\pi\pi$ in perturbative QCD approach, Phys. Rev. D **95,** 056008 (2017).

[7] J. Chai, S. Cheng, Y. h. Ju, D. C. Yan, C. D. Lü, and Z. J. Xiao, Charmless two-body B meson decays in perturbative QCD factorization approach, arXiv:2207.04190.

[8] W. Wang, Y. M. Wang, D. S. Yang, and C. D. Lu, Charmless two-body $B_{(s)} \to VP$ decays in soft-collinear-effective-theory, Phys. Rev. D **78,** 034011 (2008).

[9] H. Y. Cheng, C. W. Chiang, and A. Kuo, Updating $B \to PP, VP$ decays in the framework of flavor symmetry, Phys. Rev. D **91,** 014011 (2015).

[10] S. Zhou, Q. Zhang, W. Lyu, and C. Lü, Analysis of charmless two-body B decays in factorization assisted topological amplitude approach, Eur. Phys. J. C **77,** 125 (2017).

[11] LHCb Collaboration, Search for direct *CP* violation in charged charmless $B \to PV$ decays, arXiv:2206.02038.

[12] J. H. Alvarenga Nogueira, I. Bediaga, T. Frederico, P. C. Magalhães, and J. Molina Rodriguez, Suppressed $B \to PV$ *CP* asymmetry: *CPT* constraint, Phys. Rev. D **94,** 054028 (2016).

[13] R. Aaij *et al.* (LHCb Collaboration), Amplitude Analysis of the Decay $\bar{B}^0 \to K_S^0\pi^+\pi^-$ and First Observation of the *CP* Asymmetry in $\bar{B}^0 \to K^*(892)^-\pi^+$, Phys. Rev. Lett. **120,** 261801 (2018).

[14] I. Bediaga and C. Göbel, Direct *CP* violation in beauty and charm hadron decays, Prog. Part. Nucl. Phys. **114,** 103808 (2020).

[15] M. Beneke and M. Neubert, QCD factorization for $B \to PP$ and $B \to PV$ decays, Nucl. Phys. **B675,** 333 (2003).

[16] M. Wirbel, B. Stech, and M. Bauer, Exclusive semileptonic decays of heavy mesons, Z. Phys. C **29,** 637 (1985); M. Bauer, B. Stech, and M. Wirbel, Exclusive nonleptonic decays of D, D_s, and B mesons, Z. Phys. C **34,** 103 (1987); **34,** 103 (1987).

[17] M. Beneke, G. Buchalla, M. Neubert, and C. T. Sachrajda, QCD Factorization for $B \to PP$ Decays: Strong Phases and *CP* Violation in the Heavy Quark Limit, Phys. Rev. Lett. **83,** 1914 (1999); QCD factorization for exclusive, nonleptonic B meson decays: General arguments and the case of heavy light final states, Nucl. Phys. **B591,** 313 (2000).

[18] H. Y. Cheng and C. K. Chua, Resolving B-*CP* puzzles in QCD factorization, Phys. Rev. D **80,** 074031 (2009).

[19] B. Aubert *et al.* (*BABAR* Collaboration), Observation of Direct *CP* Violation in $B^0 \to K^+\pi^-$ Decays, Phys. Rev. Lett. **93,** 131801 (2004).

[20] T. Aaltonen *et al.* (CDF Collaboration), Evidence for the Charmless Annihilation Decay Mode $B_s^0 \to \pi^+\pi^-$, Phys. Rev. Lett. **108,** 211803 (2012).

[21] R. Aaij *et al.* (LHCb Collaboration), Observation of the Annihilation Decay Mode $B^0 \to K^+K^-$, Phys. Rev. Lett. **118,** 081801 (2017).

[22] R. L. Workman *et al.* (Particle Data Group), Review of particle physics, Prog. Theor. Exp. Phys. **2022,** 083C01 (2022).

[23] H. Y. Cheng and C. K. Chua, QCD factorization for charmless hadronic B_s decays revisited, Phys. Rev. D **80,** 114026 (2009).

[24] G. Zhu, Implications of the recent measurement of pure annihilation $B_s \to \pi^+\pi^-$ decays in QCD factorization, Phys. Lett. B **702,** 408 (2011).

[25] K. Wang and G. Zhu, Flavor dependence of annihilation parameters in QCD factorization, Phys. Rev. D **88,** 014043 (2013).

[26] C. D. Lü, Y. L. Shen, C. Wang, and Y. M. Wang, Enhanced next-to-leading-order corrections to weak annihilation B-meson decays, arXiv:2202.08073.

[27] R. Aaij *et al.* (LHCb Collaboration), Observation of the Annihilation Decay Mode $B^0 \to K^+K^-$, Phys. Rev. Lett. **118,** 081801 (2017).

[28] H. Y. Cheng, C. W. Chiang, and C. K. Chua, Width effects in resonant three-body decays: B decay as an example, Phys. Lett. B **813,** 136058 (2021).

[29] H. Y. Cheng, C. W. Chiang, and C. K. Chua, Finite-width effects in three-body B decays, Phys. Rev. D **103,** 036017 (2021).

[30] G. J. Gounaris and J. J. Sakurai, Finite-Width Corrections to the Vector Meson Dominance Prediction for $\rho \to e^+e^-$, Phys. Rev. Lett. **21,** 244 (1968).

[31] B. Aubert *et al.* (*BABAR* Collaboration), Dalitz plot analysis of $B^+ \to \pi^+\pi^+\pi^-$ decays, Phys. Rev. D **79,** 072006 (2009).

[32] H. Y. Cheng, *CP* violation in $B^\pm \to \rho^0\pi^\pm$ and $B^\pm \to \sigma\pi^\pm$ decays, arXiv:2005.06080.

[33] H. Y. Cheng, C. K. Chua, and K. C. Yang, Charmless hadronic B decays involving scalar mesons: Implications to the nature of light scalar mesons, Phys. Rev. D **73,** 014017 (2006).

[34] J. Charles, A. Höcker, H. Lacker, S. Laplace, F. R. Le Diberder, J. Malclés, J. Ocariz, M. Pivk, and L. Roos (CKMfitter Group), *CP* violation and the CKM matrix: assessing the impact of the asymmetric B factories, Eur. Phys. J. C **41,** 1 (2005), updated results and plots available at: http://ckmfitter.in2p3.fr.

[35] H. Y. Cheng and C. K. Chua, Branching fractions and *CP* violation in $B^- \to K^+K^-\pi^-$ and $B^- \to \pi^+\pi^-\pi^-$ decays, Phys. Rev. D **102,** 053006 (2020).

[36] H. Y. Cheng, C. K. Chua, and A. Soni, Final state interactions in hadronic B decays, Phys. Rev. D **71,** 014030 (2005).

[37] H. Y. Cheng, C. K. Chua, K. C. Yang, and Z. Q. Zhang, Revisiting charmless hadronic B decays to scalar mesons, Phys. Rev. D **87,** 114001 (2013).